Research in Pharmaceutical Sciences, December 2021; 16(6): 660-673
Received: 01-12-2020
Peer Reviewed: 31-01-2021
Revised: 16-04-2021
Accepted: 02-10-2021
Published: 15-10-2021

School of Pharmacy & Pharmaceutical Sciences
Isfahan University of Medical Sciences

*Original Article*

# Characterization and distribution of niosomes containing ursolic acid coated with chitosan layer

**Andang Miatmoko[1,2,*], Shofi Ameliah Safitri[1], Fayruz Aquila[1], Devy Maulidya Cahyani[1], Berlian Sarasitha Hariawan[1], Eryk Hendrianto[2], Esti Hendradi[1], and Retno Sari[1]**

*[1]Department of Pharmaceutical Sciences, Faculty of Pharmacy, Universitas Airlangga, Nanizar Zaman Joenoes Building, Campus C Mulyorejo, Surabaya, 60115, Indonesia.*
*[2]Stem Cell Research and Development Center, Universitas Airlangga, Institute of Tropical Disease Center Building, Campus C Mulyorejo, Surabaya, 60115, Indonesia.*

## *Abstract*

**Background and purpose:** Ursolic acid (UA) exhibits anti-hepatocarcinoma and hepatoprotective activities, thus promising as an effective oral cancer therapy. However, its poor solubility and permeability lead to low oral bioavailability. In this study, we evaluated the effect of different ratios of Span® 60-cholesterol-UA and also chitosan addition on physical characteristics and stability of niosomes to improve oral biodistribution.
**Experimental approach:** UA niosomes (Nio-UA) were composed of Span® 60-cholesterol-UA at different molar ratios and prepared by using thin layer hydration method, and then chitosan solution was added into the Nio-UA to prepare Nio-CS-UA.
**Findings/Results:** The results showed that increasing the UA amount increased the particle size of Nio-UA. However, the higher the UA amount added to niosomes, the lower the encapsulation efficiency. The highest physical stability was achieved by preparing niosomes at a molar ratio of 3:2:10 for Span® 60, cholesterol, and UA, respectively, with a zeta-potential value of -41.99 mV. The addition of chitosan increased the particle size from 255 nm to 439 nm, as well as the zeta-potential value which increased from -46 mV to -21 mV. Moreover, Nio-UA-CS had relatively higher drug release in PBS pH 6.8 and 7.4 than Nio-UA. In the *in vivo* study, the addition of chitosan produced higher intensities of coumarin-6-labeled Nio-UA-CS in the liver than Nio-UA.
**Conclusion and implications:** It can be concluded that the ratio of Span® 60-cholesterol-UA highly affected niosomes physical properties. Moreover, the addition of chitosan improved the stability and drug release as well as oral biodistribution of Nio-UA.

***Keywords:*** Biodistribution; Cancer; Chitosan: Coumarin-6; Niosomes; Ursolic acid.

## INTRODUCTION

Ursolic acid (UA) is a pentacyclic triterpenoid compound and also a secondary metabolite of plants, obtained from the bark, leaves, or fruit skin (1) The mechanisms underlying its anticancer effects comprise the inhibition of tumorigenesis and cancer cell proliferation, apoptosis modulation, prevention of cell cycle arrest, and autophagy occurrence (2). Furthermore, it induces protein stress and apoptosis through the mitochondria-mediated pathway (3).

Based on the *in vivo* results of the study in mice, UA possesses hepatoprotective properties which maintain the integrity of liver organ structure, reduce high levels of bilirubin, stabilize serum protein concentrations (albumin and globulin), and suppresses stress oxidation, inflammation, and apoptosis in the liver (4,5). Moreover, it has been reported that UA has low toxicity and minimal side effects, even considered as safe (6). Previous studies reported that, at certain doses, UA exerts a chemosensitization effect on cancer cells (7).

*Corresponding author: A. Miatmoko
Tel: +62-315933150, Fax: +62-315935249
Email: andang-m@ff.unair.ac.id

**Access this article online**

**Website:** http://rps.mui.ac.ir

**DOI:** 10.4103/1735-5362.327512

Based on the data obtained from acute toxicity tests, the $LD_{50}$ of UA present in mice subjects through oral administration amounted to 8,330 mg/Kg body weight (BW). However, no toxicity was detected by the chronic test at a dose of 500 mg/kg BW for 30 days (8). Phase 1 clinical trials have been carried out, namely; the tolerability and toxicity tests of UA liposomes (9). The results indicated that vital signs, such as blood pressure, body temperature, and the respiratory rate remained within normal ranges. Furthermore, the hematological and electrocardiographic parameters were also normal. While UA did not affect the patient's immune function, their side effects were reported to include fever, increased levels of gamma-glutamyl transpeptidase, and abdominal distension.

UA is included in the class IV biopharmaceutics classification system as a compound with poor solubility and permeability (10) which limits its clinical use as a treatment for various diseases. Therefore, it is necessary to develop a proper delivery system in order to increase its bioavailability. This research focuses on the modification of UA delivery in oral chemotherapy for the treatment of liver cancer, employing niosomes as drug carriers.

Niosomes constitute a carrier system that encapsulates the drug in a vesicle consisting of non-ionic surfactants as a bilayer structure and cholesterol as a stabilizer (11). The structure of niosomes is similar to that of liposomes since it is composed of non-ionic surfactants, such as sorbitan or polysorbates, which are combined with cholesterol (11). This amphiphilic bilayer structure increases drug bioavailability with low solubility in water by trapping the drug inside the structure and enabling penetration of biological membranes, thus enhancing its therapeutic effectiveness (12). An important component of niosomes is the amount and type of non-ionic surfactant used since this affects the percentage of drug encapsulation efficiency (EE) (13).

The research of Abdelaziz *et al.* into norfloxacin development found that the niosomes increase drug efficacy (14). Norfloxacin has the same properties as UA, namely; biopharmaceutics classification system class IV (15). Furthermore, previous studies have reported the use of niosomes in the paclitaxel formulation, thereby increasing their bioavailability (16). It is also stated that EE is improved as the cholesterol concentration increases and the use of Span® 60 as a surfactant due to its high transition temperature. Therefore, it is expected that niosomes increase UA bioavailability.

In the previous studies, the use of chitosan to modify UA liposomes as an antitumor therapy was reported to reduce both drug dosages and side effects, produce a controlled release profile, and enhance liposomes stability within the blood circulatory system, due to a positive charge on the liposomes surface, thereby preventing vesicle aggregation (17). Chitosan is a natural polysaccharide formed by chitin deacetylation (18). Chitosan interacts ionically between the positive charge of the amino groups and the negative charge on the cell surface (19). Furthermore, it is able to open the tight junctions of intestinal epithelial cells and produce a paracellular pathway through the barrier, resulting in higher penetration of the systemic circulation (20). Therefore, it is anticipated that oral administration of UA with chitosan coating facilitates the entry of niosomes into the blood circulation system. In this research, niosomes have been developed to provide more economically used and stable drug carriers against gastrointestinal environments than liposomes for oral chemotherapy. The physicochemical characterization of UA niosomes was carried out at different Span® 60-cholesterol-UA ratios, both with and without the addition of chitosan. Furthermore, a UA niosome biodistribution study for liver cancer therapy-induced by N-nitrosodiethylamine was conducted *via* the oral route with coumarin-6 as labeling in mice. The use of coumarin-6 as a labeling agent indicates the high efficiency and stability of encapsulation in nanoparticles with the result that free coumarin-6 was unable to penetrate cells. Therefore, the measured intensity and fluorescence levels reflect the nanoparticle levels found in cells. With the chitosan coating, the niosomes pass freely through the tight junctions and accumulate at high concentrations in the liver as the target tissue.

## MATERIALS AND METHODS

### *Materials*

The materials used in this research included UA at a purity of ≥ 90% (Sigma-Aldrich, Tokyo, Japan), cholesterol (Wako Pure Chemical Industries, Ltd., Osaka, Japan), Span® 60 (Wako Pure Chemical Industries, Ltd., Osaka, Japan), 19 centipoise (cps) chitosan (Biotech, Cirebon, Indonesia), coumarin-6 (J&K Scientific, Beijing, China), chloroform (Merck, Darmstadt, Germany), methanol (Merck, Darmstadt, Germany), sodium chloride (Merck, Darmstadt, Germany), hydrochloric acid (Merck, Darmstadt, Germany), N-nitrosodiethylamine (Sigma-Aldrich, Tokyo, Japan), and acetonitrile (Sigma-Aldrich, Tokyo, Japan). If not stated otherwise, the reagents and materials used were of non-technical grade.

### *Preparation of niosomes loading UA*

At first, cholesterol and Span® 60 were dissolved in chloroform, while UA was dissolved in methanol. Niosome-loading UA (Nio-UA) was prepared with various drug-surfactant-cholesterol mole ratios, as shown in Table 1. UA was then passively trapped in the niosomes using a thin-film method by completely evaporating the organic solvents using a rotary vacuum evaporator. The lipid film was then hydrated by adding phosphate-buffered saline (PBS) pH 7.4 to a round bottom flask and rotated at a speed of 120 rpm for 1 h at 60 °C in order to obtain a nano-suspension preparation. Furthermore, a vortex was produced to homogenize the dispersion of the thin-lipid layer and continued with sonication in a water bath for approximately 15 min. Further analysis was conducted which included particle size, zeta-potential evaluation, EE, and physical stability testing.

Following this stage, a solution of 0.1% w/v chitosan in 0.1 M acetic acid was added to the Nio-UA suspension and vortexed to produce Nio-UA with chitosan layers (Nio-UA-CS). The niosomes were subsequently separated from the free chitosan by means of the Sephadex® G-50 column.

### *Characterization of Nio-UA and Nio-UA-CS*

*Vesicle size and zeta-potential*

The particle size and polydispersity index (PDI) of Nio-UA were measured using the dynamic light scattering (DLS) method with a Delsa™ Nano C particle analyzer at 25 °C. The Nio-UA samples were diluted in Aqua Demineralizzata. Furthermore, zeta-potential measurement was also carried out using the electrophoretic light scattering method.

*EE%*

EE was evaluated by separating the Nio-UA from the free drug by centrifugation at 1,000 rpm for 10 min at 25 °C. The free UA settled at the bottom of the centrifuge tube, while the supernatant constituted the niosome fraction. Furthermore, sample preparation was conducted by adding methanol to the Nio-UA at a ratio of 2:1 (v/v). The mixture was sonicated for 5-10 min at 25 °C until completely dissolved and subsequently filtered using a 0.2 µm nylon filter membrane. The analysis was performed using high-performance liquid chromatography (HPLC). Based on the results obtained, the EE was further calculated using equation 1 (21):

$$EE\ (\%) = \frac{The\ total\ of\ AU\ trapped}{The\ total\ of\ AU\ (AU\ trapped + AU\ free)} \quad (1)$$

**Table 1.** Formulation of Nio-UA prepared at different molar ratios of Span® 60, cholesterol, and UA.

| Formulas | Molar ratio | | |
|---|---|---|---|
| | Span® 60 | Cholesterol | UA |
| SK11-UA3 | 48 | 52 | 3 |
| SK11-UA5 | 48 | 52 | 5 |
| SK11-UA10 | 48 | 52 | 10 |
| SK32-UA3 | 60 | 40 | 3 |
| SK32-UA5 | 60 | 40 | 5 |
| SK32-UA10 | 60 | 40 | 10 |
| SK61-UA3 | 84 | 16 | 3 |
| SK61-UA5 | 84 | 16 | 5 |
| SK61-UA10 | 84 | 16 | 10 |

Nio-UA, Niosomes loading ursolic acid.

*Physical stability test*

The sedimentation, flocculation, and turbidity as stability parameters were observed. The preparations were stored at 4 °C and visual observations were made qualitatively from the side of the tube, after storage on day 14 (22).

*Fourier-transform infrared spectroscopy of liposomes*

Fourier-transform infrared (FTIR) profiles of niosomes were analyzed using an FTIR spectrophotometer (ECO-ATR Bruker Alpha II, Germany). The samples were examined at wavenumbers of 4,000-450 $cm^{-1}$. The results were then compared to the literature.

*Evaluation of niosome vesicles morphology by scanning electron microscopy*

In order to evaluate the morphology of the vesicles, the niosomes i.e. Nio-UA and Nio-UA-CS were air-dried onto scanning electron microscopy (SEM) stubs with carbon tape by sputter-coating with iridium at a thickness of 20 nm to eliminate electron charging. SEM images were then taken on the SEM.

***In vitro* drug *release* study**

The UA release study of the niosomes involved the use of a dialysis method. The niosome samples were inserted into the Spectra Por® dialysis membrane (MWCO = 3.5 kDa; Spectrum Laboratories, Inc., California, USA), then placed into a medium containing 0.1% Tween® 80 in order to maintain the sink conditions (17). This test was carried out at 37 ± 0.5 °C and 400 rpm using a media release with the following conditions: for the gastric pH medium, the simulations used a 0.1 N hydrochloric acid solution pH 1.2; for the intestinal pH medium, the simulations used a PBS solution pH 6.8; and for blood pH medium the simulations used a PBS solution pH 7.4. Furthermore, sampling was carried out at a certain point during each collection when a buffer solution was added to the release medium in order to maintain the sink condition.

The concentration of the drug released was determined by HPLC at a wavelength of 210 nm. Due to the media dilution during the test process, the amount of UA released was corrected by the equation factor (2) as shown in the following equation (23):

$$Cn = C'n + \frac{a}{b}\sum_{i=1}^{n-1} Cs \quad (2)$$

where, Cn is the percentage of drug released at time point n after correction; C'n, percentage drug release measured at time point n before correction; Cs, percentage drug release at measured time point n-1; a, the volume of sample taken (mL); b, the volume of released media (mL).

***Analysis of UA levels by HPLC method***

The UA levels were determined using the HPLC method as reported in previous studies (17). It was analyzed using a ZORBAX Eclipse XDB-C18 column (Agilent Technologies, California, United States) 4.6 × 150 mm, 5µm in dimension. The mobile phase employed acetonitrile: 0.5% acetic acid (90:10 v/v) in a column at a temperature of 8 °C and a flow rate of 1.0 mL/min. Analysis was subsequently performed at a measurement wavelength (λ) of 210 nm. The linear calibration curve was prepared within the UA level range of 6-200 µg/mL with a correlation coefficient of 0.9991.

***In vivo drug biodistribution study***

Nio-UA biodistribution evaluation was conducted using mice subjects, based on the study protocol entitled "Biodistribution study of Ursolic Acid Niosomes in Mice" that has been approved by the Animal Care and Use Committee of the Faculty of Veterinary, Airlangga University with an Ethical Clearance No. 2.KE.022.02.2020.

This research used 6-week old male Balb/c mice (*Mus musculus*) weighing 20-25 g. The animals were selected randomly and divided into two groups, 6 each. The first group was given coumarin-6 labeled Nio-UA (Nio-UA-Cou6), while coumarin-6 labeled Nio-UA-CS (Nio-UA-CS-Cou6) was administered to the members of the second. The Nio-UA-Cou6 and Nio-UA-CS-Cou6 were prepared by adding about 0.3 mg coumarin-6 into the formula presented in Table1 and then produced by the same preparation method.

Before treatment, the subjects were induced with cancer by administering

N-nitrosodiethylamine intraperitoneally at a dose of 25 mg/kg BW once a week for five weeks. The evaluation of cancer induction was carried out by weighing the subjects every week during the test period in order to detect any changes. They were then given Nio-UA orally at a dose equivalent to UA 16 mg/kg BW twice a day for two days. The subjects were then sacrificed on the third day. After being anesthetized by means of 10 mg of ketamine, administered intraperitoneally, and the taking of a blood sample through the inferior vena cava, the mice subjects' spines were dislocated.

The blood samples were inserted into a tube and centrifuged at 15,000 rpm for 10 min at 4 °C to obtain plasma which was then stored at -80 °C until further analysis was performed. The evaluation of coumarin-6 levels in plasma was completed using a fluorometer at λex = 475 nm and λem = 500-550 nm using GloMax® microplate reader (Promega Corporation, USA). The linear calibration curve was prepared within the coumarin-6 level range of 0.01-0.50 µg/mL with a correlation coefficient of 0.9999. The organs including heart, lungs, liver, lymph, and kidneys were excised, removed from any adherent blood, and stored at -20 °C for analysis. They were subsequently used to produce cryosection preparations at -20 °C with a slice thickness of 3 µm (Leica CM 1960). The evaluation involved observing the tissue slices through a fluorescent microscope to quantify the niosomes accumulation in each organ. The observations were made by comparing the photomicrographs of normal, untreated control organs with those of the subjects whose organs had been administered with samples of Nio-UA-Cou6 and Nio-UA-CS-Cou6.

### *Statistical analysis*

The data obtained from the formulation parameters consisted of particle size, zeta-potential, EE, and physical stability test which constituted the mean value of three replications. The results are presented as mean ± standard deviation (SD). In order to identify the significant difference between the values contained in the data, a statistical analysis was carried out using a one-way ANOVA test, followed by HSD. In order to determine the effect of chitosan on the characteristics of drug release from niosomes and its levels in plasma, the data was statistically analyzed using the independent sample t-test method. The resulting *P*-value < 0.05 confirmed a statistically significant difference.

## RESULTS

### *Physical characteristics of UA niosomes*

Based on the evaluation of UA niosome particle size, the average results were in the range of 210.1-685.07 nm, as shown in Table 2. The addition of Span® 60, cholesterol, and UA affected niosome particle size. The SK11 had a relatively larger particle size than SK61 and SK32. A greater increase in particle size was also observed in the UA0 formula compared to those in the UA3, UA5, and UA10. The addition of UA increased the relative particle size. Furthermore, the PDI value of UA niosomes was in the range of 0.184-0.478. The formula with a PDI value less than 0.3 indicated a homogeneous system (24). The formulas with a PDI value below 0.3 were subsequently identified as SK32-UA0, SK32-UA10, SK61-UA0, and SK61-UA3.

**Table 2.** Physical properties including particle size, polydispersity index, zeta-potential, and encapsulation efficiency of Nio-UA prepared at different molar ratios of Span® 60, cholesterol, and UA.

| Formula | Physical characteristics | | | |
|---|---|---|---|---|
| | Particle size (nm) | Polydispersity index | Zeta-potential (mV) | Encapsulation efficiency (%) |
| SK11-UA3 | 263.4 ± 51.5 | 0.37 ± 0.06 | -15.76 ± 5.54 | 28.81 ± 9.26 |
| SK11-UA5 | 782.6 ± 133.5 | 0.37 ± 0.05 | -11.90 ± 2.98 | 34.76 ± 5.87 |
| SK11-UA10 | 344.2 ± 129.8 | 0.46 ± 0.06 | -22.84 ± 4.27 | 12.89 ± 2.19 |
| SK32-UA3 | 416.1 ± 59.3 | 0.41 ± 0.06 | -7.61 ± 1.86 | 29.37 ± 3.70 |
| SK32-UA5 | 305.6 ± 18.5 | 0.36 ± 0.02 | -23.02 ± 4.22 | 21.05 ± 3.41 |
| SK32-UA10 | 260.0 ± 12.0 | 0.29 ± 0.03 | -39.21 ± 7.01 | 16.40 ± 3.34 |
| SK61-UA3 | 240.3 ± 49.9 | 0.16 ± 0.02 | -27.77 ± 7.04 | 29.08 ± 6.50 |
| SK61-UA5 | 312.1 ± 41.2 | 0.32 ± 0.03 | -20.56 ± 5.11 | 16.23 ± 3.57 |
| SK61-UA10 | 234.5 ± 18.2 | 0.34 ± 0.04 | -13.01 ± 1.91 | 11.84 ± 1.00 |

Nio-UA, Niosomes loading ursolic acid.

The zeta-potential measurement results showed that the average value of niosome charge was negative as shown in Table 2. The measurement of UA EE in the niosomes showed that the more UA was added, the greater the reduction in EE. The SK11 formula with a Span® 60-cholesterol ratio of 1:1 produced the different EE diagrams. With the addition of 5 mol% UA (SK11-UA5), the value of the EE was higher than with the addition of 3 mol% UA (SK11-UA3).

A physical test was also performed to visually predict stability in the system as observed in the sediment formation occurring during 14 days of storage at 4 °C, as presented in Fig. 1. The formulas that produced the lowest sediment were SK61-UA5 and SK32-UA10. When related to the zeta-potential measurement which indicated the stability of the UA niosome system of the SK32-UA10 formula demonstrated the greatest stability compared to others. This was strengthened by the results of visually observing the sediment formed between day 0 and day 14 which was relatively stable and less than that of other formulas (data not shown). Taking all the formulas into account, those demonstrating the lowest degree of sedimentation was SK32-UA10, and this formula was used for further evaluations.

### *Characterization of UA niosomes with chitosan coating*

After the addition of chitosan, an evaluation of the particle size, zeta-potentials, PDI, and EE of UA in the niosomes was completed, the results of which are shown in Fig. 2A-F. Based on observations, the particle size of Nio-UA-CS, at 439.3 ± 25.6 nm, was greater than that of Nio-UA, at 255.1 ± 15.3 nm. With this addition, the system's PDI value increased from 0.298 ± 0.047 to 0.565 ± 0.060. The addition of chitosan to the sample also increased the zeta-potential value from -46.23 ± 3.56 mV to -20.89 ± 10.32 mV. Furthermore, the UA EE in the niosomes obtained was relatively low, namely; 16.0% and 11.8% for Nio-UA and Nio-UA-CS, respectively, which Nio-UA-CS was prepared from Nio-UA.

In addition, the SEM images show that the addition of the chitosan layer in Nio-UA-CS resulted in fewer spheroidal vesicles than that without chitosan coating (Nio-UA) as presented in Fig. 3. Physical stability was also observed after chitosan coating. Niosome stability was observed on day 7 after preparation. On day 7, the sediment was presented in a smaller amount for the Nio-UA-CS than that of Nio-UA (data not shown).

### *Spectroscopic analysis of UA niosomes*

According to the infrared spectroscopy analysis, it has been shown that UA has specific absorption bands of an alcohol group (-OH stretching: 2924 $cm^{-1}$), high intensity of carbonyl spectra absorption (-C=O: 1695 $cm^{-1}$), and an aromatic ring (C=C: 1455 $cm^{-1}$) as shown in Fig. 4. On the other hand, spectra measurement of niosomes components, such as Span® 60 showed specific bands of hydroxyl groups (-OH), alkyl groups (-CH), and esters (R-CO-OR') at 3425, 2918, and 1738 $cm^{-1}$, respectively. While, cholesterol had absorption bands of hydroxy groups (-OH: 3447 $cm^{-1}$), aromatic carbon (CH-CH: 2931 $cm^{-1}$), and carboxylate group (R-CO-OH: 1704 $cm^{-1}$). The measurement of chitosan spectra showed that it has absorption bands of -OH, primary -NH, and -C-O-C-, and C-N at 3433, 3433 (overlapped), 1155, and 1323 $cm^{-1}$, respectively.

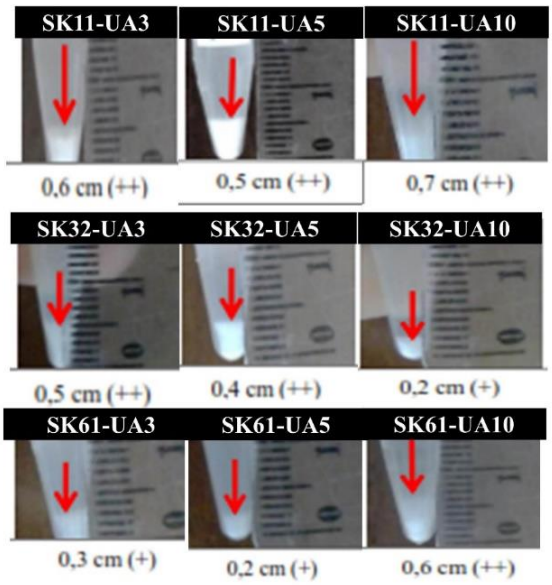


**Fig. 1.** Physical stability of niosomes loading UA prepared at different ratios of Span® 60, cholesterol, and UA at days 14 after preparation and stored at cool temperature (2-8 °C). UA, Ursolic acid.

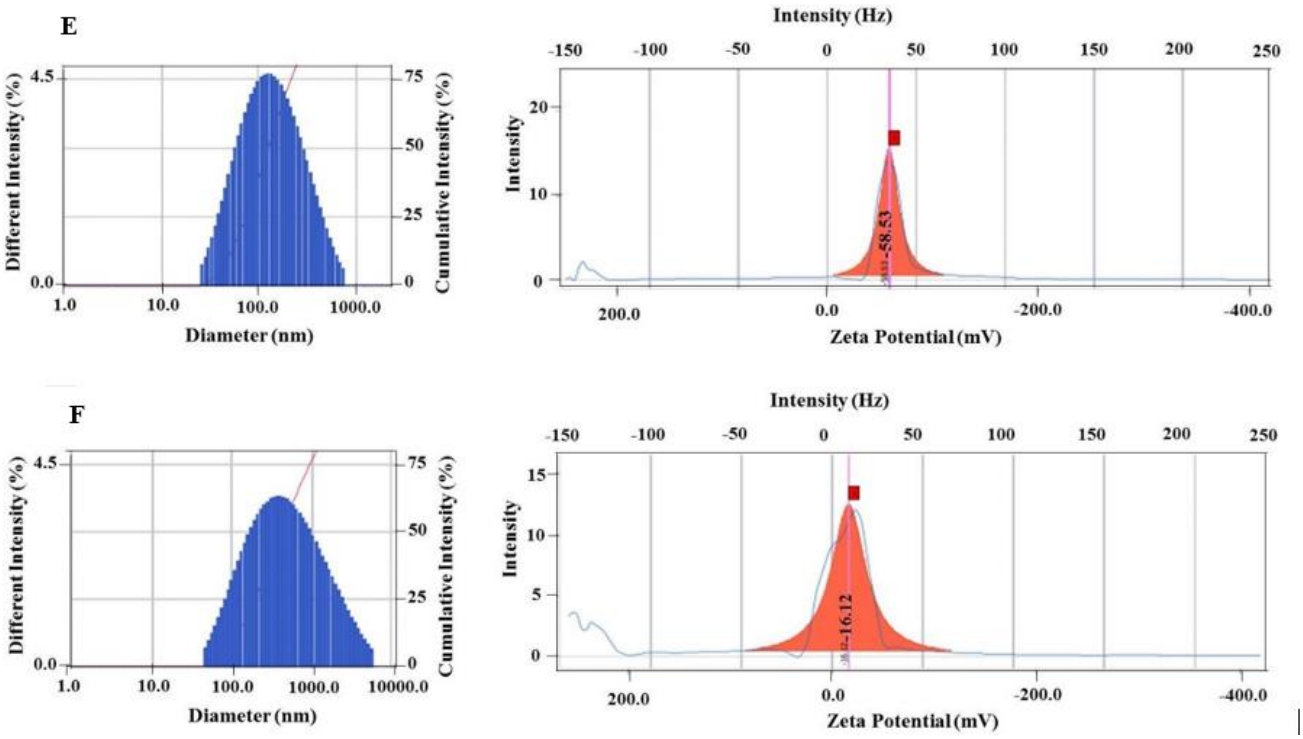


**Fig. 2.** Physical characteristics including (A) particle size, (B) polydispersity index, (C) zeta-potential, and (D) encapsulation efficiency of Nio-UA prepared at a molar ratio of cholesterol:Span® 60:UA= 60:40:10 (SK32-UA10) before and after addition of chitosan, (E) intensity distribution of particle and (F) zeta-potentials of Nio-UA and Nio-UA-CS determined by Delsa™ Nano C particle analyzer at 25 °C. n = 3, **P* < 0.05 indicates significant differences. Nio-UA-CS, Ursolic acid niosomes with chitosan layers.

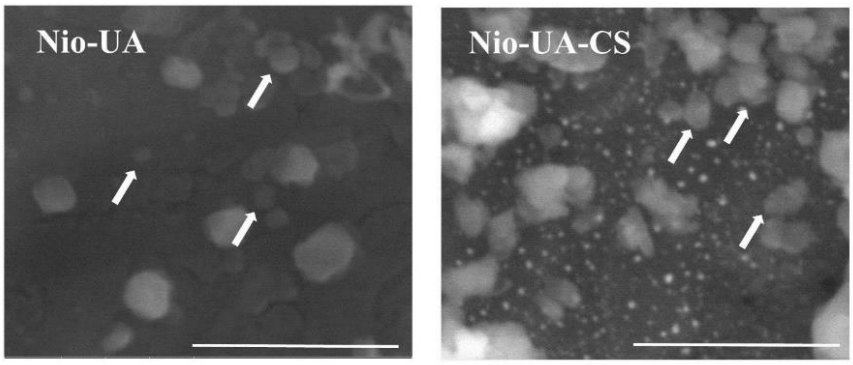


**Fig. 3.** Scanning electron photomicroscopy of niosomes loading ursolic acid without (Nio-UA) and with chitosan addition (Nio-UA-CS). Scale bar = 5 µm. White arrows indicate the vesicles.

After niosomes formation with chitosan coating, as presented in Fig. 4, the overlay results of the Nio-UA-CS spectra confirmed the presence of several identical absorption bands of the constituent components; UA, Span® 60, cholesterol, chitosan, and Nio-UA, with absorption appearing only in the Nio-UA and chitosan spectra. However, there were differences in the absorption band intensity of several of the lower and higher functional groups after the formation of Nio-UA-CS when compared to some of its constituent components. These differences were observed in the alkyl groups (CH: 3000-2850 $cm^{-1}$, CH deformation: 1350-1470 $cm^{-1}$), esters (R-CO-OR': 1740-1710 $cm^{-1}$), choline (N-$CH_3$: 980-940 $cm^{-1}$), and carboxylate (R-CO-OH: 1315-1270 $cm^{-1}$) which had a lower intensity than their constituent components, while the carboxylic acid functional groups (C=C aromatic: 1550-1400 $cm^{-1}$) had a higher absorption band.

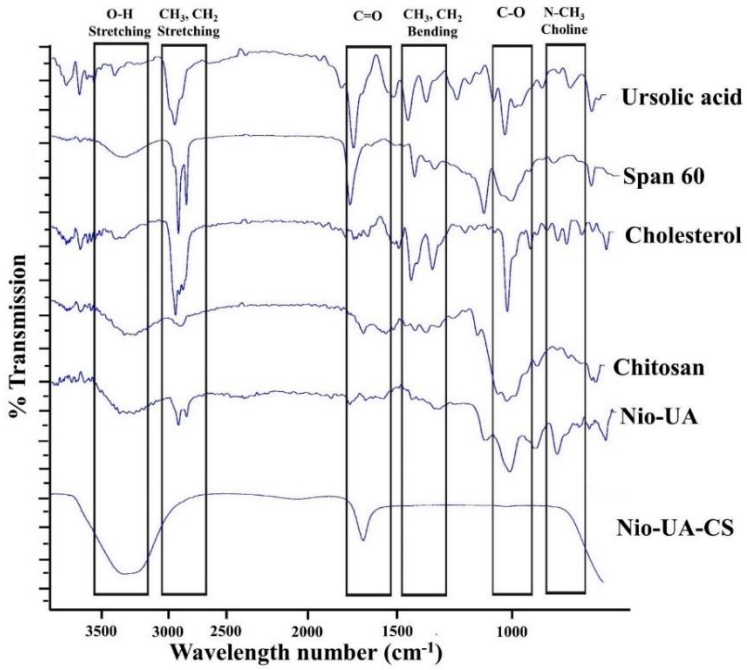


**Fig. 4.** Profiles of Fourier transform infrared spectra of niosomal components, niosomes loading ursolic acid without (Nio-UA) and with chitosan addition (Nio-UA-CS).

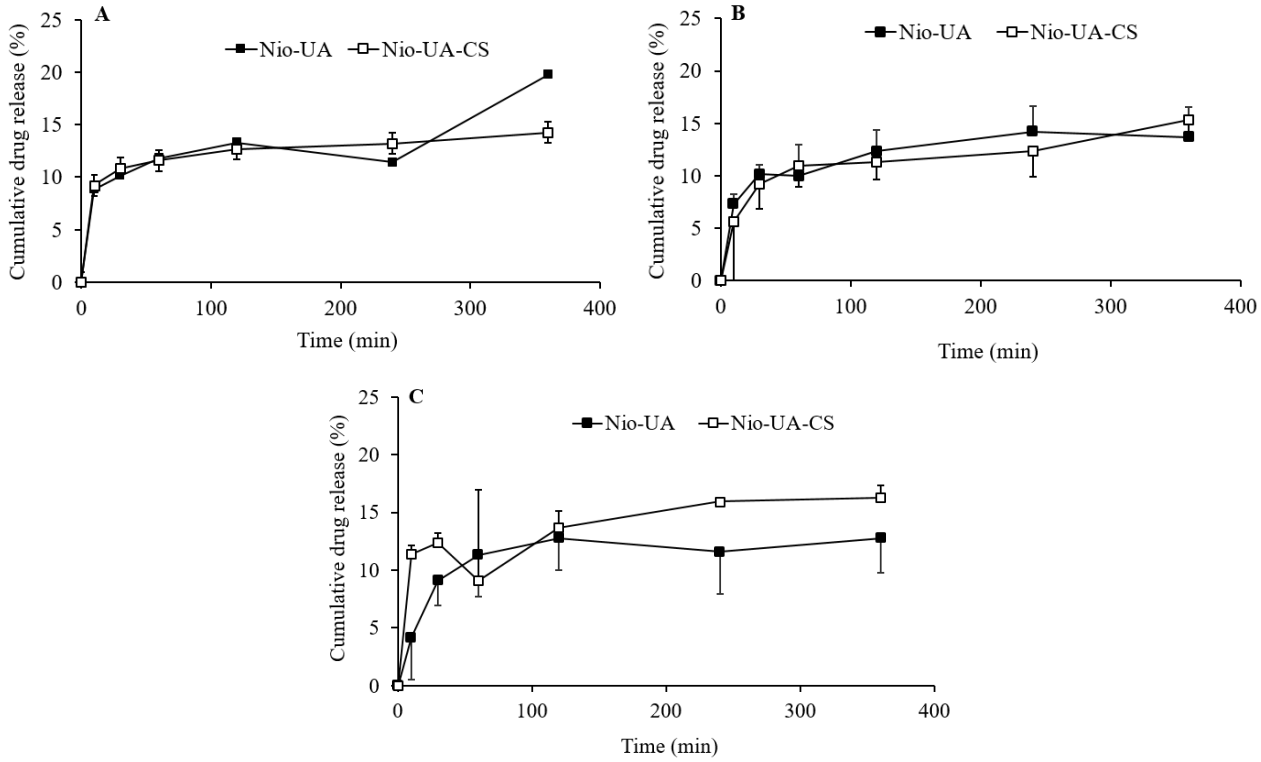


**Fig. 5.** *In vitro* drug release from niosomal ursolic acid without (Nio-UA) and with chitosan addition (Nio-Chit-UA) at drug release media pH (A) 1.2, (B) 6.8, and (C) 7.4.

### *In vitro release of UA from niosomes with chitosan layers*

The evaluation of UA release from the niosomes was carried out at three different pH media because the intended route of the drug use was oral. The release test results are presented in Fig. 5A-C. The cumulative UA release from Nio-UA after the test lasting 360 min was 19.77% on 0.1 N HCl pH 1.2, 13.67% on PBS pH 6.8, and 12.76% on PBS pH 7.4 media. Meanwhile, the cumulative UA released from Nio-UA-CS was 14.27% in 0.1 N

HCl pH 1.2, 15.29% in PBS pH 6.8, and 16.27% in PBS pH 7.4 media. Based on these results, the relatively high cumulative drug release for Nio-UA has occurred at gastric pH 1.2. However, the findings of the statistical analysis indicated no significant difference between the release results in these three pH media. The amount of UA released from Nio-UA-CS on 0.1 N HCl pH 1.2 medium was relatively lower than that of Nio-UA. In contrast, at pH 6.8 and 7.4, the UA release efficiency of Nio-UA-CS was greater than Nio-UA.

### *In vivo biodistribution of UA niosomes*

The results of the coumarin-6 level measurements in the plasma of the Nio-UA and Nio-UA-CS groups with coumarin-6 labeling, i.e. Nio-UA-Cou6 and Nio-UA-CS-Cou6, respectively, are presented in Fig. 6. These results indicated an increase in coumarin-6 levels on plasma indicating that Nio-UA-CS increased niosome levels compared to Nio-UA. The coumarin-6 level measurement in plasma in the Nio-UA-Cou6 group (0.12 ± 0.044 µg/mL), was significantly lower than those of the Nio-UA-CS-Cou6 group (1.85 ± 0.155 µg/mL).

The photomicroscopy observation results of organs after sample treatment with coumarin-6 labeling are shown in Fig. 7. The results showed that Nio-UA-Cou6 was distributed to the heart in the subjects highlighted in green, which was produced by the fluorescence of coumarin-6. However, there was no difference in intensity between the two, nor in the results of the observations relating to the lungs, lymph, and kidneys.

However, a qualitative difference in coumarin-6 fluorescence intensity was found between Nio-UA and Nio-UA-CS. The Nio-UA-CS-Cou6 showed a very high intensity compared to Nio-UA-Cou6 in the liver. The high fluorescence intensity indicated that Nio-UA-CS delivered more drugs to the liver by oral administration.

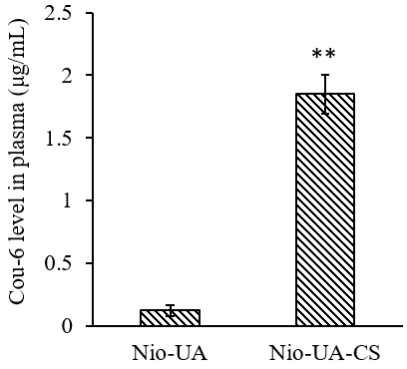


**Fig. 6.** Mean plasma level of coumarin-6 in mice after administration of Nio-UA-Cou6 and Nio-UA-CS-Cou6 at a dose of 64 mg UA/kg body weights per oral. The dose was divided twice a day for two days. $^{**}P < 0.01$ Indicates significant difference. Nio-UA-CS-Cou6, Ursolic acid niosomes with chitosan layers labeled with coumarin-6.

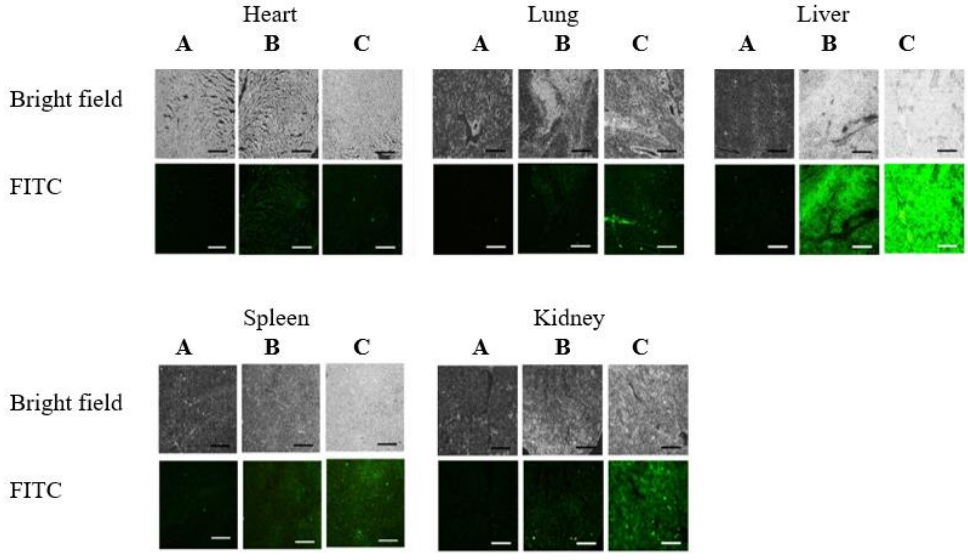


**Fig. 7.** Photomicrographs of heart, lung, liver, spleen, and kidney tissue of (A) control and treatment groups and taken at 24 h after the second drug administration of (B) coumarin-6 labeled ursolic acid niosomes, (C) coumarin-6 labeled ursolic acid niosomes with chitosan layer. The tissue sections were observed with a fluorescence microscope. Scale bar: 100 µm.

## DISCUSSION

In this study, the development of UA niosomes was affected with a different ratio of Span® 60-cholesterol-UA. The purpose of this study was to increase the effectiveness of UA as oral chemotherapy which was found to have low water solubility, short plasma half-life, and poor permeability (10).

UA niosomes were prepared with different mole ratios of Span 60-cholesterol-UA. Based on the obtained results, the average value of UA niosomes particle size was in the range of 210.1-685.1 nm. The addition of cholesterol and UA showed a tendency to increase the particle size of the niosomes, due to the increase in rigidity of the bilayer in the liquid phase (25). Furthermore, the effect of UA filling the space in the hydrophobic membrane increased the particle size of the niosomes. The Span® 60 also had a long-saturated alkyl chain i.e. $C_{16}$ which generally involved larger vesicle dimensions (26). In addition to the particle size, PDI values of UA niosomes are also needed to be considered. From the research results, PDI niosomes loading UA was in the range 0.184-0.478. A formula that had a PDI value less than 0.3, demonstrated the homogeneity and monodispersed conditions of the system (24), as the homogeneous niosome particles enhanced the expected therapeutic efficacy.

In addition to the particle size and PDI, the zeta-potential value also played a role in predicting carrier system stability (24). According to the research conducted by Kharia *et al*. the zeta-potential value more than |30 mV rendered the system more stable because the repulsive force between particles prevented aggregation (27). The SK32-UA10 formula indicated a zeta-potential value less than -30 mV (-41.99 mV) leading to the conclusion that the niosomes were stable because there was considerable electrostatic stabilization (24). Moreover, the addition of UA did not always increase the zeta-potential value.

With regard to the successful drug delivery, the efficiency of UA niosome encapsulation played an important role in indicating the amount of drug that was to be delivered. The larger the moles % UA added, the greater the decrease in EE. Furthermore, it had also been reported in previous paclitaxel liposome studies that the effect of increasing the amount of drug administered affected their physical properties including aggregation and particle size. The higher the amount of drug trapped, the more rapidly the instability of the system accelerates as confirmed by the formation of post-sonication aggregates observed (28), with the exception of the SK11-UA5 formula which had a higher EE compared to SK11-UA3. The effect that occurred was based on structure formation. Niosomes were created in bilayer consisted of double chain structures in which the single tail surfactant was mixed with cholesterol-formed vesicles. Based on its molecular shape and solubility, cholesterol was a relatively rigid lipid that assisted in the formation of the bilayer vesicle by filling the space between the amphiphilic layers, thereby strengthening the structure formed (29). In the niosome bilayer membrane, UA was trapped between Span® 60 molecules and cholesterol. The different spaces in each formula resulted in each vesicle membrane having limited free space capacity within which to trap UA. This could be observed from the graphs of SK11, SK61, and SK32 indicating a decrease in EE with each additional UA amount. However, the niosome formulation in SK11-UA5 consisting of Span® 60 and cholesterol at a mol ratio of 1:1 resulted in a higher EE. This increase represented a significant value compared to other formulas. The rise in the EE value of the SK11-UA5 formula also affected the particle size value. This large EE value occurred because the addition of cholesterol to the formula affected the hydrophobic membrane layer, with the cholesterol competing with the drug to occupy space in the bilayer (26).

In this research, the formula demonstrating the optimum physicochemical parameters was SK32-UA10 with a relatively smaller particle size of 243.2 nm and PDI of 0.289, indicating that the system was homogeneous and monodispersed. Furthermore, it had a zeta-potential value of -41.99 mV with sediment formed up to day 14 which was relatively stable and less than other formulas (unpublished data). Another parameter, namely; the addition of UA 10 mol% produced

an EE value of 12.95%, indicating that UA was trapped in a higher amount than with other formulas. Another feature to be considered was the physical stability of the niosomes which constituted the main problem affecting drug delivery. Therefore, it was necessary to take measures to increase the physical stability of the lipid vesicles, for example, rendering the system in a dispersed form within a thicker medium. Furthermore, molecular analysis was also performed to predict the nature of the UA encapsulation model and its effect on niosome stability.

After chitosan coating, the particle size of Nio-UA-CS was larger than that of Nio-UA. This was due to the chitosan accumulating on the niosome surface through electrostatic and hydrophobic interactions (30), which was in accordance with the previous research postulating that the addition of chitosan to niosomes progressively increases vesicle size (31). However, following the addition, the PDI value increased from 0.298 ± 0.047 to 0.565 ± 0.060 indicating that Nio-UA-CS was more heterogeneously distributed. The increase in PDI after the addition of chitosan was due to the formation of a random polymer layer on the vesicle surface (31). Furthermore, this was considered to be due to the formation of hydrogen bonds in the phosphate and phospholipid carbonyl groups resulting from a shift in the absorption band to a lower wavenumber. Because there was no dominant shift or new band formation in the Nio-UA-CS spectra, the new compound formation did not occur. The only interactions were the physical ones between functional groups involving hydrogen bonds.

The addition of chitosan to the sample increased the zeta-potential value of Nio-UA-CS. This rise was due to the increased positive density charge in the surface of niosome vesicles caused by interaction between chitosan and niosome vesicles (17). The relatively low efficiency of niosome encapsulation, due to the passive loading of the drug encapsulation method, meant that not all of the UA was entrapped in the vesicles.

The stability of Nio-UA-CS was superior to that of Nio-UA due to the presence of charged compounds in the membrane and steric stabilizers which reduce vesicle aggregation (22). The results obtained indicated that the highest drug release of Nio-UA samples was at gastric pH 1.2. However, the statistical analysis performed confirmed no significant difference between the drug amounts released from the three different pH media. This was due to the hydrophobic characteristics of UA (log P = 7.4) which strengthen the bond between Span® 60 (log P = 6.9) and cholesterol (log P = 7.1) as the constituent components of niosomes. Therefore, the difference in pH media did not affect the UA released. Furthermore, UA released from Nio-UA-CS in 0.1 N HCl pH 1.2 media was less than those from Nio-UA. This was due to increased niosome stability and the presence of chitosan layers which effectively prevented drug leakage. Moreover, the chitosan layer was firmly bound to the niosome surface, thereby slowing drug release (17). In contrast, at pH 6.8 and 7.4, the cumulative UA release of Nio-UA-CS was greater than that of Nio-UA. This process occurred at the pH indicated because the $-NH_2$ group of chitosan was protonated which produced swelling of Nio-UA-CS. As a result, UA molecules were easily separated from the niosome vesicles (17).

Based on the findings of this research, the addition of chitosan increased the particle size, zeta-potential, and PDI of UA, while also enhancing the niosomes' physical stability. Furthermore, the addition of chitosan also increased the release of UA niosomes at alkaline pH. However, it was necessary to analyze the interaction of chitosan with UA niosomes and the efforts to produce a smaller particle size of Nio-UA-CS in order to obtain a niosome formulation with appropriate chitosan as a form of oral chemotherapy.

Following the photomicroscopy results, by using a fluorescent microscope with a fluorescein isothiocyanate (FITC) filter, it was found that UA niosomes had accumulated in all organs. Due to physiological factors and the possibility of phagocytosis by macrophages, the UA niosomes accumulated to a greater extent in the liver. Numerous studies have shown that nanoparticles were distributed to almost all tissues and organs with their relative concentrations dependent upon the characteristics of nanoparticles and their

interactions within the body (32). Nanoparticle accumulation in the body was influenced by its stability and surface characteristics such as zeta-potential. The nanoparticles with a positive charge caused non-specific accumulation which was distributed across several organs such as the liver (33). In the liver, particles were generally accumulated in large quantities through the role of Kupffer cells, hepatocytes, and endothelial cells (32). In the case of liver tumors, such as those caused by N-nitrosodiethylamine, the accumulation of nanoparticles was greater in these organs through the passive targeting which forms part of the enhanced permeability and retention effect (34). The high accumulation levels in the liver were also caused by the phagocytosis of macrophages where this organ represented the main route for the metabolism and excretion of nanoparticles (32). This was because nanoparticles were widely phagocytosed by macrophages in the liver and lymph organs (16). In addition, nanoparticle accumulation in the lymphatic system was elevated due to the role of the marginal zone and red pulp. Moreover, macrophages and dendritic cells may have also contributed to this accumulation (32).

The results showed that UA niosomes were distributed in the plasma and the subjects' organs as evidenced by the level and intensity of coumarin-6. High levels of Nio-UA-CS were accumulated in the liver. Based on the findings of this research, the chitosan coating on UA niosomes increased their *in vivo* biodistribution in plasma and mice organs using coumarin-6 labeling. However, the correlation between coumarin-6 and UA levels as an active ingredient in therapy has not been confirmed by this research. Therefore, further study of UA values is required. Moreover, it is necessary to determine UA levels in plasma and organs to prove the role of chitosan coating in increasing UA niosome biodistribution.

## CONCLUSION

This research investigated the effect of differences in the Span® 60-cholesterol-UA ratio on the physicochemical characteristics of niosomes, including particle size, zeta-potential, EE, and physical stability. Based on the results obtained, the difference in the Span® 60-cholesterol-UA ratio affected the physicochemical characteristics of UA niosomes. Furthermore, UA niosomes with robust physical stability had a mole percent ratio of 3:2:10, with a potential zeta value of -41.99 mV. Meanwhile, the addition of cholesterol increased the particle size, membrane stabilization, and EE of the niosomes. Subsequently, the addition of chitosan increased the particle size, zeta-potential, and PDI of the niosomes, in addition to their physical stability during storage. Therefore, the addition of chitosan affected the release characteristics of the UA niosomes. Given the *in vivo* study results, it can be asserted that the presence of chitosan layers increased the level of UA niosomes in plasma to the coumarin-6 level and its qualitative distribution in the liver.

### *Acknowledgements*

This study was financially supported by a Preliminary Research on Excellence in Higher Education Institutions (Penelitian Dasar Unggulan Perguruan Tinggi, PDUPT) through Grant No. AMD/E1/KP.PTNBH/2020 and 710/UN3/14/PT/2020 provided by the Ministry of Research and Technology-National Research and Innovation Agency of the Republic of Indonesia.

### *Conflict of interest statement*

The authors declared no conflicts of interest in this study.

### *Authors' contribution*

A. Miatmoko contributed to the concept and design of study and acquisition, analysis, and interpretation of data, drafting the article and revising the article critically for important intellectual content; S.A. Safitri, F. Aquila, D.M. Cahyani, and B.S. Hariawan acquired, analyzed, and interpreted the data, drafted and revised the article critically for important intellectual content; E. Hendrianto and R. Sari drafted and revised the article critically for important intellectual content. The final version of the article for publication has been approved by all authors.

## REFERENCES


1. Wozniak L, Skapska S, Marszałek K. Ursolic acid-a pentacyclic triterpenoid with a wide spectrum of pharmacological activities ursolic acid-a pentacyclic triterpenoid with a wide spectrum of pharmacological activities. Molecules. 2015;20(11):20614-20641. DOI: 10.3390/molecules201119721.
2. Seo DY, Lee SR, Heo J, No M, Rhee BD, Ko KS, *et al*. Ursolic acid in health and disease. Korean J Physiol Pharmacol. 2018;22(3):235-248. DOI: 10.4196/kjpp.2018.22.3.235.
3. Hyu MH, Kao TC, Yen GC. Oleanolic acid and ursolic acid induce apoptosis in HuH7 human hepatocellular carcinoma cells through a mitochondrial-dependent pathway and downregulation of XIAP. J Agric Food Chem. 2010;58(10):6110-6118. DOI: 10.1021/jf100574j.
4. Gharibi S, Bakhtiari N, Moslemee-Jalalvand E, Bakhtiari F. Ursolic acid mediates hepatic protection through enhancing of anti-aging biomarkers. Curr Aging Sci. 2018;11(1):16-23. DOI: 10.2174/1874609810666170531103140.
5. Ma JQ, Ding J, Zhang L, Liu C. Protective effects of ursolic acid in an experimental model of liver fibrosis through Nrf2/ARE pathway. Clin Res Hepatol Gastroenterol. 2015;39(2):188-197. DOI: 10.1016/j.clinre.2014.09.007.
6. Geerlofs L, He Z, Xiao S, Xiao ZC. Repeated dose (90 days) oral toxicity study of ursolic acid in Han-Wistar rats. Toxicol Rep. 2020;7:610-623. DOI: 10.1016/j.toxrep.2020.04.005.
7. Kim G, Kan S, Kang H, Lee S, Ko HM, Kim JH, *et al*. Ursolic acid suppresses cholesterol biosynthesis and exerts anti-cancer effects in hepatocellular carcinoma cells. Int J Mol Sci. 2019;20(19):4767,1-15. DOI: 10.3390/ijms20194767.
8. Li Y, Xing D, Chen Q, Chen WR. Enhancement of chemotheraputic agent-induced apoptosis by inhibition of NF-kB using ursolic acid. Int J Cancer. 2010;127(2):462-673. DOI: 10.1002/ijc.25044.
9. Qian Z, Wang X, Song Z, Zhang H, Zhou S, Zhao J, *et al*. A phase I trial to evaluate the multiple-dose safety and antitumor activity of ursolic acid liposomes in subjects with advanced solid tumors. Biomed Res Int. 2015;2015:809714,1-7. DOI: 10.1155/2015/809714.
10. Eloy JO, Saraiva J, de Albuquerque S, Marchetti JM. Preparation, characterization and evaluation of the *in vivo* trypanocidal activity of ursolic acid-loaded solid dispersion with poloxamer 407 and sodium caprate. Braz J Pharm Sci. 2015;51(1):101-109. DOI: 10.1590/S1984-82502015000100011.
11. Shatalebi MA, Mostafavi SA, Moghaddas A. Niosome as a drug carrier for topical delivery of N-acetyl glucosamine. Res Pharm Sci. 2010;5(2):107-117. PMID: 21589799.
12. Hajizadeh MR, Maleki H, Barani M. *In vitro* cytotoxicity assay of D-limonene niosomes : an efficient nano-carrier for enhancing solubility of plant-extracted agents. Res Pharm Sci. 2019;14(5):448-458. DOI: 10.4103/1735-5362.268206.
13. Mirzaei M, Dadashzadeh S, Monavari H, Ebrahimi S. Preparation and characterization of acyclovir loaded nano-niosomes as a potential antiviral drug delivery system. Res Pharm Sci. 2012;7(5):S232.
14. Abdelaziz AA, Elbanna TE, Sonbol FI, Gamaleldin NM, Maghraby GM El. Optimization of niosomes for enhanced antibacterial activity and reduced bacterial resistance: *in vitro* and *in vivo* evaluation. Expert Opin Drug Deliv. 2015;12(2):1-18. DOI: 10.1517/17425247.2014.942639.
15. Bhattacharya B, Mondal A, Soni SR, Das S, Bhunia S, Bal Raju K, *et al*. Multidrug salt forms of norfloxacin with non-steroidal anti-inflammatory drugs: solubility and membrane permeability studies. CrystEngComm. 2018;20(41):6420-6429. DOI: 10.1039/C8CE00900G.
16. Sezgin-Bayindir Z, Beşikci A, Yüksel N. Paclitaxel-loaded niosomes for intravenous administration: pharmacokinetics and tissue distribution in rats. Turk J Med Sci. 2015;45(6):1403-1412. PMID: 26775401.
17. Wang M, Zhao T, Liu Y, Wang Q, Xing S, Li L, *et al*. Ursolic acid liposomes with chitosan modification: promising antitumor drug delivery and efficacy. Mater Sci Eng C Mater Biol Appl. 2017;71:1231-1240. DOI: 10.1016/j.msec.2016.11.014.
18. Szymańska E, Winnicka K. Stability of chitosan-a challenge for pharmaceutical and biomedical applications. Mar Drugs. 2015;13(4):1819-1846. DOI: 10.3390/md13041819.
19. Moghassemi S, Hadjizadeh A. Nano-niosomes as nanoscale drug delivery systems: an illustrated review. J Control Release. 2014;185:22-36. DOI: 10.1016/j.jconrel.2014.04.015.
20. Wang M, Liu M, Xie T, Zhang B, Gao X. Chitosan-modified cholesterol-free liposomes for improving the oral bioavailability of progesterone. Colloids Surfaces B Biointerfaces. 2017;159:580-585. DOI: 10.1016/j.colsurfb.2017.08.028.
21. Miatmoko A, Salim RH, Zahro SM, Annuryanti F, Sari R, Hendradi E. Dual loading of primaquine and chloroquine into liposome. Eur Pharm J. 2019;66(2):18-25. DOI: 10.2478/afpuc-2019-0009.
22. Junyaprasert VB, Teeranachaideekul V, Supaperm T. Effect of charged and non-ionic membrane additives on physicochemical properties and stability of niosomes. AAPS PharmSciTech. 2008;9(3):851-859. DOI: 10.1208/s12249-008-9121-1.
23. Aronson H. Correction factor for dissolution profile calculations. J Pharm Sci. 1993;82(11):1190-1190. DOI: 10.1002/jps.2600821126.
24. Mohsen AM, AbouSamra MM, ElShebiney SA. Enhanced oral bioavailability and sustained delivery of glimepiride *via* niosomal encapsulation: *in-vitro* characterization and *in-vivo* evaluation. Drug Dev Ind Pharm. 2017;43(8):1254-1264. DOI: 10.1080/03639045.2017.1310224.

25. Essa EA. Effect of formulation and processing variables on the particle size of sorbitan monopalmitate niosomes. Asian J Pharm. 2010;4(4):227-233. DOI: 10.4103/0973-8398.76752.
26. Fathalla D, Abdel-Mageed A, Abdel-Hamed F, Ahmed M. *In-vitro* and *in-vivo* evaluation of niosomal gel containing aceclofenac for sustained drug delivery. Int J Pharm Sci Res. 2014;1:105-115. DOI: 10.15344/2394-1502/2014/105.
27. Kharia AA, Singhai AK, Verma R. Formulation and evaluation of polymeric nanoparticles of an antiviral drug for gastroretention. Int J Pharm Sci Nanotech. 2012;4(4):1557-1562. DOI: 10.37285/ijpsn.2011.4.4.6.
28. Khan MI, Madni A, Ahmad S, Mahmood MA, Rehman M, Ashfaq M. Formulation design and characterization of a non-ionic surfactant based vesicular system for the sustained delivery of a new chondroprotective agent. Braz J Pharm Sci. 2015;51(3):607-615. DOI: 10.1590/S1984-82502015000300012.
29. Abdelkader H, Alani AWG, Alany RG. Recent advances in non-ionic surfactant vesicles (niosomes): self-assembly, fabrication, characterization, drug delivery applications and limitations. Drug Deliv. 2014;21(2):87-100. DOI: 10.3109/10717544.2013.838077.
30. Hasan M, Ben Messaoud G, Michaux F, Tamayol A, Kahn C, Belhaj N, *et al*. Chitosan-coated liposomes encapsulating curcumin: study of lipid-polysaccharide interactions and nanovesicle behavior. RSC Adv. 2016;6(51):45290-45304. DOI: 10.1039/C6RA05574E.
31. Rinaldi F, Hanieh PN, King L, Chan N, Angeloni L, Passeri D, *et al*. Chitosan glutamate-coated niosomes: a proposal for nose-to-brain delivery. Pharmaceutics. 2018;10(2):38-53. DOI: 10.3390/pharmaceutics10020038.
32. Li M, Al-Jamal KT, Kostarelos K, Reineke J. Physiologically based pharmacokinetic modeling of nanoparticles. ACS Nano. 2010;4(11):6303-6317. DOI: 10.1021/nn1018818.
33. Ge X, Wei M, He S, Yuan W. Advances of non-ionic surfactant vesicles (niosomes) and their application in drug delivery. Pharmaceutics. 2019;11(2):55-70. DOI: 10.3390/pharmaceutics11020055.
34. Yu B, Hsu S, Zhou C, Wang X, Terp MC, Wu Y, *et al*. Lipid nanoparticles for hepatic delivery of small interfering RNA. Biomaterials. 2012;33(25):5924-5934. DOI: 10.1016/j.biomaterials.2012.05.002.